Progress In Electromagnetics Research, PIER 55, 209–226, 2005

SCATTEING OF MULTILAYER CONCENTRIC ELLIPTICAL CYLINDERS EXCITED BY SINGLE MODE SOURCE

S. C. Hill and J. M. Jarem

University of Alabama in Huntsville
Huntsville, AL 35899, USA

Abstract—The Electromagnetic (EM) fields of a concentric, mismatched-material, elliptical system are studied when excited by an interior or exterior electric surface current. The interior or exterior surface current is assumed to be proportional to a single, angular Mathieu mode. It is shown that despite the fact that the system is concentric, that a single Mathieu mode surface current excites EM Mathieu-mode fields of all orders. A derivation of the EM fields due a single mode electric surface in an infinite, homogeneous media is given, as well as the matrix formulation from which the EM fields of the mismatched-material, elliptical system may be determined. Validation of numerical results and comparison with other research work is given for both interior and exterior single-mode, current sources. Detailed numerical examples of the EM fields that result for a single-mode, exterior source excitation are given for the first time. Discussion of the EM mode coupling that results by single-mode excitation on a mismatched elliptical system is given.

1. INTRODUCTION

An important problem in Electromagnetics (EM) is determining the EM scattering that arises from both homogeneous elliptical cylindrical objects and inhomogeneous ones whose permittivity and permeability are functions of position inside the object. Many results have been obtained for scattered EM field expansions in Mathieu functions [1, 2] which are functions of the elliptical cylinder coordinates, including closed form expressions for the expansion coefficients for the homogeneous, perfectly conducting elliptical cylinder [3] and references therein. An exact Mathieu series solution for plane wave scattering from a homogeneous dielectric elliptical cylinder has been obtained by [4, 5]. Scattering from a dielectric-coated elliptic cylinder has been investigated [6] and scattering from a spatially uniform, dielectric-coated impedance elliptical cylinder has recently been studied [7]. An exact (formal) solution to transverse-magnetic excitation of multilayer dielectric elliptical cylinders has been obtained using a recursive procedure [8]. Plane wave scattering of multilayer, isorefractive, elliptical cylinders was studied using a matrix based recursive solution [9]. The exact solution to plane wave scattering of a single isorefractive elliptic cylinder had earlier been obtained [10].

An interesting feature of EM scattering from elliptical, cylindrical cylinders of mismatched dielectric permittivity and mismatched magnetic permeability values is the fact that when an EM field which is proportional to a single Mathieu mode is incident on the system, that the scattering due to this mode causes the excitation of EM fields proportional to Mathieu modes of different order than that of the incident EM field. This has been as shown in [11, 12] when an interior, single mode Mathieu electric current source excited EM fields in a mismatched elliptical system. This situation is quite different from that when a circular EM mode is incident on a concentric, mismatched, multilayer system of circular cylinders (each layer of the system is assumed homogeneous). In this system a circular EM mode incident on the system will induce only circular modes of the same order. In studies of scattering from both circularly shaped objects [13, 14] and elliptically shaped objects [4, 8], the Radar Cross Section (RCS) of the system is usually the quantity of most interest, and thus a plane wave excitation is the one that is most often used. Since a plane wave in circular and elliptical coordinates is a superposition of an infinite number of modes, when calculating the RCS for circular or elliptically shaped objects, it is difficult to gain a sense of how each mode of the plane wave excitation is coupled to each mode of the scattered EM field. This is particularly true for RCS calculations for elliptically

shaped objects, since each elliptical mode in the plane wave excitation, excites or couples to, all other elliptical modes in the scattered field.

The purpose of this paper is to study in mismatched-material, elliptical systems, the EM fields which are excited by single, Mathieu-mode elliptical source. The excitation source will be located either interior to or exterior to the elliptical cylinders and will be, for simplicity, assumed to be symmetric in the x and y directions. The excited EM fields will be determined by expanding these fields in series of products of angular and radial Mathieu functions of unknown amplitude, and then by using the method of moments, solving for the EM unknown field amplitudes.

The EM fields due to a single-mode interior source in a mismatched elliptical system were first calculated in [11, 12]. In [11, 12] the focus of the work was not to develop a Mathieu mode-matching algorithm, but was to develop a numerical procedure entitled the Rigorous Coupled Wave Analysis (RCWA) algorithm for inhomogeneous elliptical systems. This RCWA algorithm was used to solve EM scattering problems for concentric elliptical cylinder systems whose material parameters of dielectric permittivity and magnetic permeability varied spatially. The elliptical mode-matching algorithm to be described herein was used in [11, 12] only to check numerical results of the RCWA algorithm when the elliptical shells of the system were homogeneous materials. The focus of the present paper will be to present in detail the Mathieu mode matching algorithm which was used in [11, 12] and will be to present new results of how a single Mathieu-mode exterior source excites EM fields in a mismatched elliptical system. The work presented herein is based on the masters thesis work [15] performed by one of the authors, Susan C. Hill. The Mathieu function numerical calculations to be presented in the paper were made by the algorithms of [16].

The present authors feel that the analysis of this paper will be very useful to researchers who wish to investigate scattering from elongated, possibly thin objects. By adjusting the eccentricity of the elliptical scattering system, very elongated ellipses can be constructed which then approximately represent an elongated thin or flattened scattering object (for example; a radar absorbing covered aircraft wing; a plank of wood or vegetation; (in the area of bioelectromagnetics) a finger [17] or wrist; etc.) that might be illuminated. This study will also be useful to validate EM field solutions found by other numerical methods or mathematical techniques. These include approximate diffraction methods, Finite Difference-Time Domain (FD-TD), or Finite Element (FE) methods, rigorous coupled wave analysis, and other approaches used where an exterior source is present that can be represented in

a Mathieu function series expansion. For example, the single mode elliptic source used in this paper could be used in iterative algorithm and solution developed by [18] to study TM scattering by two infinitely long lossy dielectric cylinders.

2. BASIC FORMULATION

2.1. Maxwell's Equations in Elliptical Coordinates

The elliptical geometry of the mismatched dielectric elliptical cylinders with interior and exterior sources is shown in Fig. 1. The elliptical cylindrical coordinates [1] are the angular coordinate u, $0 < u < \infty$ (in the radial direction), the angular coordinate v, $0 \leq v \leq 2\pi$, and the axial coordinate z, $-\infty < z < \infty$. Normalized coordinates [11, 12] will be used for convenience by letting $\rho = k_0\tilde{\rho}$, $x = k_0\tilde{x}$, $y = k_0\tilde{y}$,

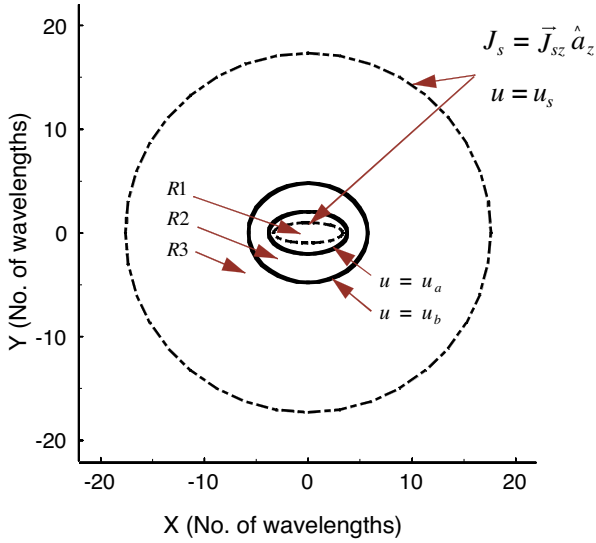

Figure 1. This figure is drawn to scale to illustrate the system geometry where $\rho = 20$, $u_a = 0.602$, $u_b = 1.198$, the interior source current is located at $u_s = 0.3$, the exterior source current is located at $u_s = 2u_b = 2.396$, and λ_0 is the free space wavelength. The three regions of the system denoted R1, R2, and R3 are each homogeneous, where; in R1, $\varepsilon_1 = 1$ and $\mu_1 = 1$; in R2, $\varepsilon_2 = 2.9851786$ and $\mu_2 = 1.4$; and in R3, $\varepsilon_3 = 1.5$ and $\mu_3 = 1.2$. The $u = u_s = 2.396$ outermost ellipse appears circular because $\rho\cosh(u) = x/\cos(v)$ and $\rho\sinh(u) = y/\sin(v)$ are very nearly equal.

$x = \rho \cosh u \cos v$, $y = \rho \sinh u \sin v$ where unnormalized coordinates $(\tilde{\rho}, \tilde{x}, \tilde{y})$ are in meters and $k_0 = 2\pi/\lambda_0$ is the free space wavenumber (1/meters) and λ_0 is the free space wavelength. The material of the system has permittivity $\tilde{\varepsilon} = \varepsilon\varepsilon_0$, where ε is the relative permittivity, and permeability $\tilde{\mu} = \mu\mu_0$, where μ is the relative permeability. The impedance of free space is, $\eta_0 = \sqrt{\mu_0/\varepsilon_0} = 377\Omega$.

The EM fields are independent of the axial coordinate z and are functions only of the u and v coordinates. In this case, Maxwell's equations in elliptical coordinates for time harmonic EM fields in a charge free, non-conducting, homogeneous medium [11, 12] are in component form given by

$$\mu\eta_0 h(u,v) H_u(u,v) = j\frac{\partial E_z(u,v)}{\partial v} \tag{1a}$$

$$\mu\eta_0 h(u,v) H_v(u,v) = -j\frac{\partial E_z(u,v)}{\partial u} \tag{1b}$$

$$\varepsilon E_z(u,v) = -\frac{j}{h^2}\left(\frac{\partial(\eta_0 h H_v)}{\partial u} - \frac{\partial(\eta_0 h H_u)}{\partial v}\right) \tag{1c}$$

where the elliptical scale factor, $h(u,v)$ is

$$h(u,v) = \frac{\rho}{\sqrt{2}}\left(\cosh 2u - \cos 2v\right)^{\frac{1}{2}}. \tag{2}$$

It is convenient to define the function $U_v(u,v)$ given by [11, 12], as

$$U_v(u,v) = \eta_0 h(u,v) H_v(u,v) = -j\frac{1}{\mu}\frac{\partial E_z(u,v)}{\partial u} \tag{3}$$

2.2. Elliptically Symmetric EM Source Fields in Uniform Space

It will be assumed that a surface current $\vec{J}_S$ which is located at u_s, excites EM fields in an infinite homogeneous medium. This surface current satisfies the boundary matching equation [11, 12]

$$\begin{aligned}\vec{J}_S &= \hat{a}_u X\left(\vec{H}^+(u_s,v,q) - \vec{H}^-(u_s,v,q)\right) \\ &= \left(H_v^+(u_s,v,q) - H_v^-(u_s,v,q)\right)\hat{a}_z = J_{SZ}(u_s,v,q)\hat{a}_z. \end{aligned} \tag{4}$$

The EM fields from this source will be treated later in the analysis as EM source fields which themselves excite scattered fields in the dielectric mismatched system in the same way that a plane wave excited EM fields in the elliptical systems of [4, 5, 8]. Here, the plus and minus signs indicate the exterior and interior of the source location.

Specifically in this study, the exciting surface current will be taken to be a sum of even angular Mathieu functions of even order [1, 11, 12]

$$J_s(u_s, v, q) = \frac{1}{h(u_s, v)} \sum_{m=0,2,\cdots}^{\infty} J_{sm} ce_m(v, q) \tag{5}$$

This source is symmetric about the x and y axes.

The EM fields excited by Eq. (5) may be expanded in products of even angular and radial Mathieu functions. The EM fields in the interior of the source may be expanded in even radial Mathieu functions of the first kind, $Mc_m^{(1)}$. The $Mc_m^{(1)}$ functions are used in the interior since they are well behaved at the origin. The EM fields inside the current source may be represented as

$$E_z^{(IN)}(u, v, q) = \sum_{m=0}^{\infty} A_m^{I-} Mc_m^{(1)}(u, q) ce_m(v, q), \qquad u < u_s \tag{6a}$$

$$U_v^{(IN)}(u, v, q) = \frac{1}{j\mu} \sum_{m=0}^{\infty} A_m^{I-} \frac{dMc_m^{(1)}(u, q)}{du} ce_m(v, q), \; u < u_s \tag{6b}$$

The constant $q = \frac{k^2\rho^2}{4}$, where $k = \sqrt{\mu\varepsilon}$ is the propagation constant, will depend on the material parameters and the geometry of the source. Outside the current source, the EM fields radiate outwardly and are given by

$$E_z^{(EX)}(u, v, q) = \sum_{m=0}^{\infty} A_m^{I+} Mc_m^{(4)}(u, q) ce_m(v, q), \qquad u_s < u \tag{7a}$$

$$U_v^{(EX)}(u, v, q) = \frac{1}{j\mu} \sum_{m=0}^{\infty} A_m^{I+} \frac{dMc_m^{(4)}(u, q)}{du} ce_m(v, q), \; u_s < u \tag{7b}$$

The EM field expansion coefficients, A_m^{I-} and A_m^{I+}, are determined; (1) by imposing the EM field boundary conditions that the tangential z component of the total electric field must be continuous at u_s, $E_z^{(IN)}(u_s, v, q) = E_z^{(EX)}(u_s, v, q)$ and 2) by requiring the tangential v component of the magnetic field at u_s to satisfy the jump discontinuity boundary condition

$$U_v^{(EX)}(u_s, v, q) - U_v^{(IN)}(u_s, v, q) = \eta_0 h(u_s, v) J_s(u_s, v, q). \tag{8}$$

These two equations are next multiplied by an infinite set of test functions, angular Mathieu functions with parameter q, and integrated over the full range of the angular coordinate v, $0 \leq v \leq 2\pi$. Next,

the EM field series expansions from Eqs. (6)–(8) are evaluated at u_s, substituted into the integrals, then after the order of integration and summation is exchanged, it is found

$$\sum_{m=0}^{\infty} \left\{ A_m^{I-} Mc_m^{(1)}(u_s, q) - A_m^{I+} Mc_m^{(4)}(u_s, q) \right\} \int_0^{2\pi} ce_m(v, q) ce_r(v, q) dv = 0, \quad r = 0, 2, \cdots \tag{9a}$$

$$\sum_{m=0}^{\infty} \left\{ A_m^{I+} \frac{dMc_m^{(4)}(u_s, q)}{du} - A_m^{I-} \frac{dMc_m^{(1)}(u_s, q)}{du} - j\mu\eta_0 J_{sm} \right\} \times \int_0^{2\pi} ce_m(v, q) ce_r(v, q) dv = 0, \qquad r = 0, 2, \cdots \tag{9b}$$

The sums in Eqs. (9a), (9b) are proportional to Kronecker deltas due to the orthogonality of angular Mathieu functions that have the same parameter q. Eqs. (9a), (9b) simplifies, and one finds infinite sets of decoupled, invertible 2×2 linear systems

$$\begin{bmatrix} 0 \\ j\eta_0 \mu J_{sr} \end{bmatrix} = \begin{bmatrix} Mc_r^{(4)}(u_s, q) & -Mc_r^{(1)}(u_s, q) \\ \dfrac{dMc_r^{(4)}(u_s, q)}{du} & -\dfrac{dMc_r^{(1)}(u_s, q)}{du} \end{bmatrix} \begin{bmatrix} A_r^{I+} \\ A_r^{I-} \end{bmatrix}, \quad r = 0, 2, \cdots \tag{10}$$

from which the unknown incident EM field expansion coefficients are determined. Once the current source expansion coefficients, J_{sr}, are specified, each 2×2 linear system can readily be solved to find A_m^{I-} and A_m^{I+} for each mode independently of all other modes [11, 12]. It is interesting to note that if only a single coefficient J_{sr} is nonzero then only the r^{th} order Mathieu mode will be excited.

2.3. Dielectric Shell Matrix Equation for an Elliptically Symmetric Source Excitation

In this section the EM fields will be solved for in three mismatched material regions when the system is excited by the elliptically symmetric surface current described in the previous section and when the current source is either in the most interior or exterior region as shown in Fig. 1. In this section the matrix formulation for the interior source will be presented in detail. The formulation for the exterior source is identical to interior except that a different excitation source matrix needs to be used. The three regions of the system are

assumed each homogeneous, with the material relative permittivities ε and relative permeabilities μ in Regions 1, 2, and 3 given in the caption of Fig. 1. The EM fields due to the surface current radiating in homogeneous space calculated in the previous section are considered to be the incident excitation fields in the more general dielectric mismatched case considered here.

We will now present the interior matrix formulation. For the interior source matrix formulation the source current is located at u_s, $0 < u_s < u_a$. In Reg. 1 outside the source current location, the EM fields are superpositions of the outwardly radiating incident EM fields and the unknown scattered EM fields. The interior fields are given by

$$\begin{aligned} E_z^{(1)}(u,v,q_1) &= \sum_{m=0}^{\infty} \left(A_m^{I+} Mc_m^{(4)}(u,q_1) + A_m^{(1)} Mc_m^{(1)}(u,q_1) \right) \\ &\quad \times ce_m(v,q_1), \qquad u_s < u < u_a \end{aligned} \tag{11a}$$

$$\begin{aligned} U_v^{(1)}(u,v,q_1) &= \frac{1}{j\mu_1} \sum_{m=0}^{\infty} \left(A_m^{I+} \frac{dMc_m^{(4)}}{du}(u,q_1) + A_m^{(1)} \frac{dMc_m^{(1)}}{du}(u,q_1) \right) \\ &\quad \times ce_m(v,q_1), \qquad u_s < u < u_a \end{aligned} \tag{11b}$$

where A_m^{I+} is given by the solution of Eq. (10) with $q = q_1$ [11, 12]. In Region 2, the unknown, scattered EM fields are inwardly and outwardly radiating, and are given by

$$\begin{aligned} E_z^{(2)}(u,v,q_2) &= \sum_{m=0}^{\infty} \left(A_m^{(2)} Mc_m^{(3)}(u,q_2) + A_m^{(3)} Mc_m^{(4)}(u,q_2) \right) \\ &\quad \times ce_m(v,q_2), \qquad u_a < u < u_b \end{aligned} \tag{12a}$$

$$\begin{aligned} U_v^{(2)}(u,v,q_2) &= \frac{1}{j\mu_2} \sum_{m=0}^{\infty} \left(A_2^{(2)} \frac{dMc_m^{(3)}(u,q_2)}{du} + A_m^{(3)} \frac{dMc_m^{(4)}(u,q_2)}{du} \right) \\ &\quad \times ce_m(v,q_2), \qquad u_a < u < u_b \end{aligned} \tag{12b}$$

In Region 3, the EM fields are unknown, outwardly radiating EM fields, and are given by

$$E_z^{(3)}(u,v,q_3) = \sum_{m=0}^{\infty} A_m^{(4)} Mc_m^{(4)}(u,q_3) ce_m(v,q_3), \quad u_b < u < \infty \tag{13a}$$

$$U_v^{(3)}(u,v,q_2) = \frac{1}{j\mu_3} \sum_{m=0}^{\infty} A_m^{(4)} \frac{dMc_m^{(4)}(v,q_3)}{du} ce_m(u,q_3), \quad u_b < u < \infty \tag{13b}$$

The unknown EM field expansion coefficients are found by matching the tangential components of the EM fields at each interface in the system as required by the EM boundary conditions. The resulting four equations are multiplied by a limited set of $2N+1$ test functions, angular Mathieu functions that have material parameters of Region 2, and then integrated over the angular coordinate v, resulting in four equations for each mode r, $r = 0, 2, \cdots, 2N$. After evaluating the EM field series expansions on the appropriate interfaces and exchanging the order of integration and summation, a system of equations is obtained for the unknown EM field expansion coefficients. For example, the $u = u_a$ electric field equation is given by the following set of $2N+1$ equations:

$$\sum_{m=0}^{\infty}\left(A_m^{I+}Mc_m^{(4)}(u_a,q_1)+A_m^{(1)}Mc_m^{(1)}(u_a,q_1)\right)\int_0^{2\pi}ce_m(v,q_1)ce_r(v,q_2)dv=$$
$$\sum_{m=0}^{\infty}\left(A_m^{(2)}Mc_m^{(3)}(u_a,q_2)+A_m^{(3)}Mc_m^{(4)}(u_a,q_2)\right)\int_0^{2\pi}ce_m(v,q_2)ce_r(v,q_2)dv,$$
$$r=0,2,\cdots,2N \qquad (14)$$

Similar interface matching equations exist for the other EM field components.

It is interesting to note that in the right hand side of Equation (14) in the angular Mathieu function overlap integral the $ce_m(v,q_2)$ functions satisfy an orthogonality relation, but in the left hand side of Eq. (14), the $ce_m(v,q_1)$ and the $ce_r(v,q_2)$ functions are not orthogonal. This occurs because $q_1 = q_2$ in the right hand side overlap integral and $q_1 \neq q_2$ on the left hand side of the equations. Thus we see in a clear and unambiguous way, that if only a single J_{sm} coefficient of Eq. (10) is excited (J_{sm} excites the A_m^{I+} incident EM field coefficient), that since the overlap integral for $q_1 \neq q_2$ is non-zero, modes other than the m^{th} mode in a dielectric mismatched system will be excited. Thus mode coupling between the source and scattered EM fields will occur in the system.

After implementing boundary conditions, a system of equations results for the unknown EM field expansion coefficients is found. The system of equations has the form

$$\begin{bmatrix} -S^{21}M_{11}^1 & S^{22}M_{21}^3 & S^{22}M_{21}^4 & 0 \\ -S^{21}U_{11}^1 & S^{22}U_{21}^3 & S^{22}U_{21}^4 & 0 \\ 0 & -S^{22}M_{22}^3 & -S^{22}M_{22}^4 & S^{23}M_{32}^4 \\ 0 & -S^{22}U_{22}^3 & -S^{22}U_{22}^4 & S^{23}U_{32}^4 \end{bmatrix} \begin{bmatrix} A^1 \\ A^2 \\ A^3 \\ A^4 \end{bmatrix}$$

$$= \begin{bmatrix} S^{21}M_{11}^{4}A^{I+} \\ S^{21}U_{11}^{4}A^{I+} \\ 0 \\ 0 \end{bmatrix} \tag{15}$$

where S^{22} is the diagonal, square block $(N+1)\times(N+1)$ angular Mathieu function overlap integral, and the matrix elements of S^{21}, for example, are given by

$$\left[S^{21}\right]_{ij} = \int_0^{2\pi} ce_i(v,q_2)ce_j(v,q_1)dv, \qquad i,j = 0,2,\cdots,2N \tag{16}$$

The Mathieu functions and their derivatives evaluated on the boundaries are diagonal square block $(N+1)\times(N+1)$ dimensional matrices with matrix elements given by, for example,

$$\left[M_{21}^{3}\right]_{ii} = Mc_i^{(3)}(u_a,q_2), \qquad i = 0,2,\cdots,2N \tag{17a}$$

and

$$\left[U_{21}^{3}\right]_{ii} = \frac{1}{j\mu_2}\frac{dMc_i^{(3)}(u_a,q_2)}{du}, \qquad i = 0,2,\cdots,2N \tag{17b}$$

The unknown EM field expansion coefficient vectors, A^1, A^2, A^3, and A^4 are $(N+1)\times(N+1)$ dimensional column sub-vectors representing overall the $4(N+1)$ unknowns in the system. The right hand side column vector represents the excitation of the surface current source in Reg. 1 with A^{I+} given as the solution of Eq. (10) with material parameters of Reg. 1.

As can be seen in Eq. (15), the system takes a particularly simple form because the angular Mathieu functions of Reg. 2 were chosen as the test functions. However, the system matrix is in general non-diagonal and non-symmetrical because the angular Mathieu functions are non-orthogonal when they depend on different parameters q_ℓ, $\ell = 1,2,3$. As a consequence, mode coupling can occur where a given mode of the incident EM fields can excite distinctly different modes in the scattered EM fields.

The EM field expansion coefficients for an exterior elliptically symmetric source (See Fig. 1) are found in the same way as for an interior elliptically symmetric source except that the right hand side vector of Eq. (15) is replaced by

$$\begin{bmatrix} 0 & 0 & -S^{23}M_{32}^{1}A^{I-} & -S^{23}U_{32}^{1}A^{I-} \end{bmatrix}^T \tag{18}$$

with A_m^{I-} given as the solution of Eq. (10) with material parameters of Region 3. The A_m^{I-} are used because the excitation current source is exterior to the dielectric shell. Mode coupling can occur in the presence of an exterior source just as in the case of an interior source since the same left hand matrix is used to determine EM field coefficients of the system.

3. NUMERICAL RESULTS FOR THE INTERIOR AND EXTERIOR ELLIPTICALLY SYMMETRIC SOURCE

This section will be concerned with presenting some numerical results of boundary matching algorithm developed in the previous sections. Two numerical cases are presented, the first case presents numerical results when the exciting surface current is interior to the dielectric shell and the second when the surface current source is exterior. Fig. 1 shows the geometry of the scattering system when the exciting elliptical surface current is placed on the interior or exterior of the mismatched elliptical dielectric shells. The elliptical geometry parameters and the material parameters (permittivity and permeability) are listed in the Fig. 1 caption. We note that Fig. 1 is drawn to the exact scale of the scattering system under investigation. As can be seen, because of the large u value of elliptical current source, the exterior elliptical current source is nearly circular in shape.

We begin by presenting numerical results of the first case when the elliptical source is located in the interior of the dielectric shell (Reg. R1) and is assumed to be excited by a single $ce_m(v, q_1)$ mode with $m = 0$ and with the surface current set to a value of $J_{SZ} = 1.0(A/m)$. In Fig. 1 the exterior source is set to zero. This numerical case has been previously analyzed in [11, 12] and is presented here as validation of the numerical methods which are used in this paper. In [11, 12] this case was studied by both by the mode matching used in this paper and was studied by using a state variable electromagnetic analysis technique, RCWA, to find the EM fields and power of the system. Table 1 shows the normalized power that results from [11] using five expansion and testing modes and the present work using seven modes. The normalized power in Table 1 is calculated at four locations namely just inside and outside the $u = u_a^{\pm}$ (R1:R2 boundary) and the $u = u_b^{\pm}$ (R2:R3 boundary). As can be seen from Table 1 extremely good power conservation holds from layer to layer as physically required since the system is lossless. We also note that the agreement from matrix methods of this paper agree very closely with that of [11], thus giving good validation of the numerical results. Fig. 2 shows a db plot of the power which is radiated individually from the different modes at

Table 1. Computed values of the normalized power that is radiated through the interfaces $u = u_a^-$, $u = u_a^+$, $u = u_b^-$, and $u = u_b^+$. The number of modes in the electromagnetic field Mathieu function expansions is different for the two calculations, but both adequately converged.

Data Source	No. Modes	P_{TOT} / P_{JS}			
		$u = u_a^-$ Region 1	$u = u_a^+$ Region 2	$u = u_b^-$ Region 2	$u = u_b^+$ Region 3
This Work	7	0.727005	0.727005	0.727005	0.727005
Ref. [Jarem 2002]	5	0.7270355	0.7270554	0.7270554	0.7271340

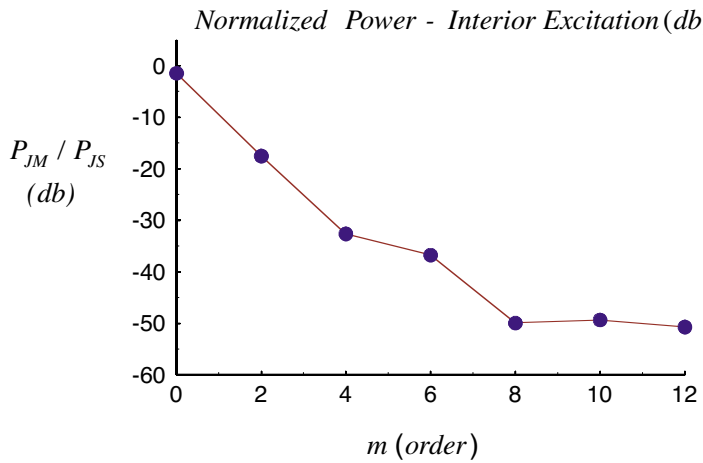

Figure 2. Shown is the normalized power P_m/P_{JS} in each Mathieu mode in Reg. 3 at $u = u_b^+$ obtained here for a seven mode EM field expansion when exited by the interior source of Fig. 1.

the $u = u_b^+$ boundary using 35 modes to calculate the EM fields of the system. As can be seen from Fig. 2, the majority of power is radiated in the lower order modes. The numerical case presented in Fig. 2 was also calculated in [11] and the results presented here agree almost exactly with those presented in [11]. This provides further validation of the algorithm presented herein.

We will now present numerical results of the second case namely when the elliptical source is located in the exterior of the dielectric shell (Reg. R3) and is assumed to be excited by single $ce_m(v, q_3)$ mode for $m = 0$ and $m = 2$. Plots of the source functions are shown in

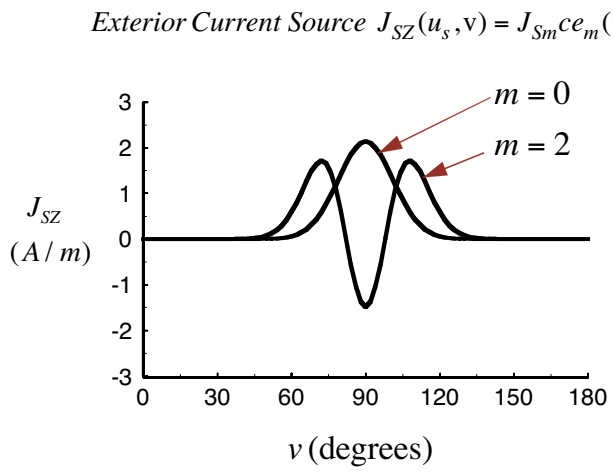

Figure 3. Shown is the exterior surface current (proportional to the angular Mathieu functions with material parameters of Reg. 3) for the $m = 0$ and $m = 2$ modes.

Fig. 3. As can be seen from Fig. 3, the $m = 0$ mode excites radiation which is fairly broadside at $v = 90°$ whereas the $m = 2$ mode excites radiation at the $v = 70°$, $90°$, and $110°$ degree locations.

Figs. 4a, b shows the real and imaginary parts of the E_z electric field (in units of (V/m)) as calculated at $u = u_b^-$ (R2:R3 interface, solid line plot) and $u = u_b^+$ (R2:R3 interface, dotted line plot) when excited by the $m = 0$ source and Figs. 4c, d show similar plots for the $\eta_0 H_v$ (in units of (V/m)) magnetic field variable. As can be seen from the Figs. 4a–d, extremely close matching of the EM fields occurred which shows that the EM boundary conditions of the system are being satisfied to a high degree of accuracy, further validating the numerical algorithm used in the paper. In observing the plots of Fig. 4, one notices for the excitation used, that the $\mathrm{Im}ag(\eta_0 H_v)$ in Fig. 4d was approximately four times larger in peak to peak magnitude than the EM fields of Figs. 4a, b, c. An interesting feature of the plots which can be clearly seen in Figs. 4a, b, c is the fact that the $\mathrm{Re}al(E_z)$, $\mathrm{Im}ag(E_z)$, and $\mathrm{Re}al(\eta_0 H_v)$ EM fields of the system are showing a high degree of constructive and destructive interference (or modal variation) in the v angular direction, despite the fact that the current source excitation consisted of a single lobe $ce_m(v, q_3)$, $m = 0$ source function (shown in Fig. 3). The fact that a high degree of constructive and destructive interference has occurred is physically reasonable since the $m = 0$ broadside wave launches a disturbance in the dielectric

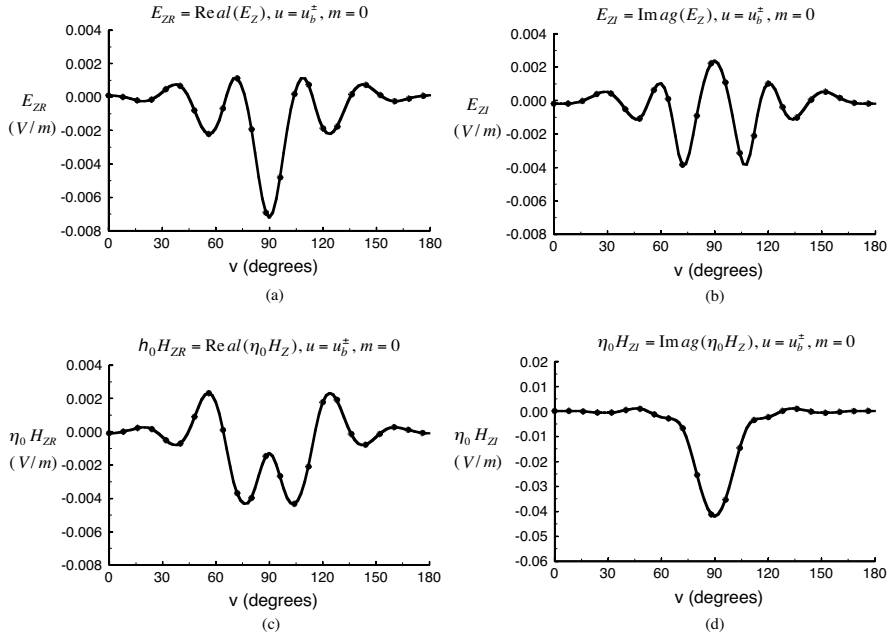

Figure 4. Shown are real and imaginary parts of the electric field E_z (Figs. a, b) and magnetic field $\eta_0 H_v$ (Figs. c, d) when evaluated on the interface at $u = u_b^{\pm}$ over the range $0 \leq v \leq 180$. Only the $m = 0$ mode of the source current is present.

shell (Reg. R2) which thus propagates radiation in the forward and backward directions causing the interference which is observed. In Fig. 4d, recalling that the peak to peak magnitude is about four times larger than in Figs. 4a, b, c, one also observes about the same level of interference in the v range ($0 < v < 60°$, $120 < v < 180°$) of Fig. 4d as seen in Figs. 4a, b, c. The interference observed in Figs. 4a–d is thus strong evidence that there has been significant excitation of the higher order Mathieu modes in the system from the exterior source.

Figs. 5a, b, c, d shows the same type of electric and magnetic field plots as were described in Figs. 4a, b, c, d except that the current source was proportional to a $ce_m(v, q_3)$, $m = 2$, mode (plotted in Fig. 3) rather than a $ce_m(v, q_3)$, $m = 0$ mode. For this excitation, strong illumination of the elliptical cylinder occurs at $v = 70°$, $v = 90°$ and $v = 110°$. As can be seen from Figs. 5a, b, c, d (as in Figs. 4a, b, c, d), extremely close matching of the EM fields has occurred, which again shows that the EM boundary conditions of the system are being satisfied to a high degree of accuracy. Again, one observes a much higher degree of

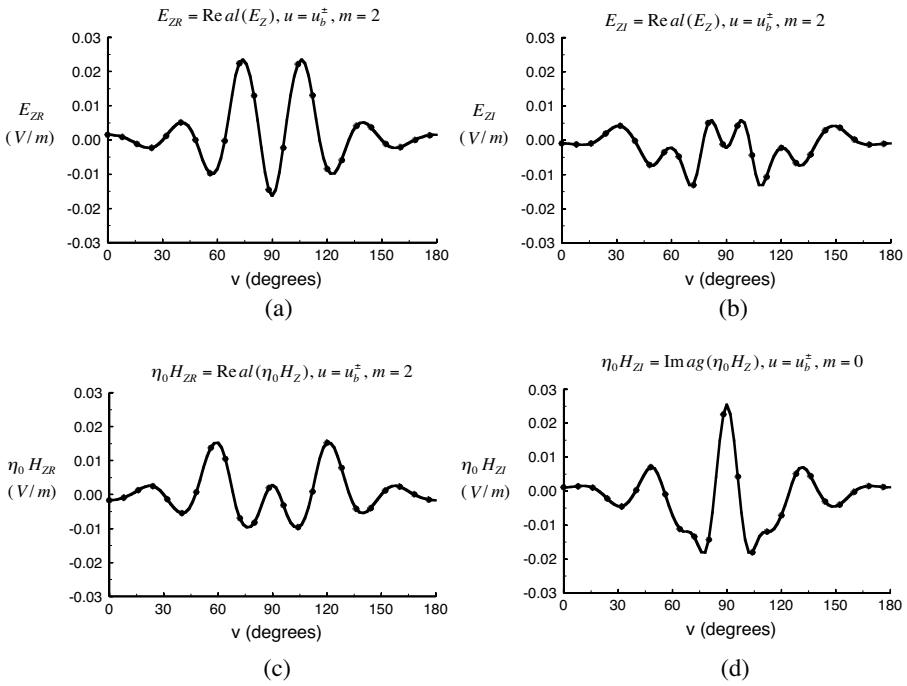

Figure 5. The same plot as Fig. 4 is shown except that $m = 2$.

constructive and destructive interference (or modal variation) in the v angular direction than was shown by the $ce_m(v, q_3),\ m = 2$ source (Fig. 3). The interference observed in Figs. 5a, b, c, d is again strong evidence that there has been significant excitation of the higher order Mathieu modes in the system by the $ce_m(v, q_3),\ m = 2$ mode exterior source.

4. CONCLUSION

In conclusion the paper has presented a electromagnetic Mathieu modal matching solution for the EM fields of an elliptical cylinder when illuminated by surface currents which are proportional to $m = 0$ and $m = 2$ interior angular Mathieu functions $ce_m(v, q_1)$ and exterior $ce_m(v, q_3)$ ones. The EM fields of the interior surface current, as determined by the present modal matching algorithm, were compared to the numerical solution by an independent numerical algorithm, namely the RCWA method [11, 12] and close matching of the solutions was observed validating the numerical calculation of the present

algorithm. Validation of the algorithm was also provided by the close agreement shown in Figs. 4 and 5 of the EM field solutions as calculated at the $u = u_b$ elliptical shell interface.

An interesting feature of the EM field solution when the excitation was an exterior source, was the fact that although the electric current sheet excitations possessed a low modal variation (proportional to $ce_m(v, q_3)$, $m = 0$, $m = 2$, see Fig. 3), the EM fields excited by these sources shown in Figs. 4 and 5 showed a high degree of constructive and destructive interference in the v angular direction. This indicated that these sources induced excitation of modes of higher order than $m = 0$ and $m = 2$. This feature is an interesting one, when compared to the scattering case of a single mode exciting a concentric circular cylindrical mismatched dielectric system. In the circular mismatched dielectric system, as mentioned in the Introduction, the m^{th} mode excites EM fields only of order m. In an elliptical mismatched system a single m^{th} order will in general excite all orders of m.

As mentioned in the Introduction, the authors feel the work presented here will also be useful to other researchers wishing to validate other numerical EM algorithms such as the finite element (FE) method, and the finite difference-time domain (FD-TD) method for example. The modal method used here is extremely accurate and converges with expansions of 35 modes.

REFERENCES

1. Abramowitz, M. and I. Stegun, *Handbook of Mathematical Functions,* Chap. 20, "Mathieu Functions," National Bureau of Standards Applied Mathematics Series 53, Ninth Printing, 1970.
2. Stratton, J., *Electromagnetic Theory,* Mcgraw-Hill, New York, NY, 1941.
3. Bowman, J., T. Senior, and P. Uslenghi, *Electromagnetic and Acoustic Scattering by Simple Shapes,* Chap. 3, "The Elliptic Cylinder," 129–180, Hemisphere Publishing Corp., New York, NY, revised printing, 1987.
4. Yeh, C., "Backscattering cross section of a dielectric elliptical cylinder," *J. Opt. Soc. Amer.,* Vol. 55, No. 3, 309–314, Mar. 1965.
5. Yeh, C., "The diffraction of waves by a penetrable ribbon," *J. Math. Phys.,* Vol. 4, No. 1, 65–71, Jan. 1963.
6. Ragheb, H. and L. Shafai, "Electromagnetic scattering from a dielectric-coated elliptic cylinder," *Can. J. Physics,* Vol. 66, 1115–1122, 1988.
7. Sebak, A., "Scattering from dielectric-coated impedance elliptical

cylinder," *IEEE Trans. on Antennas and Prop.,* Vol. 48, No. 10, 1574–1580, Oct. 2000.

8. Caorsi, S., M. Pastorino, and M. Raffetto, "Electromagnetic scattering by a multilayer elliptic cylinder under transverse-magnetic illumination: Series solution in terms of Mathieu functions," *IEEE Trans. on Antennas and Prop.,* Vol. 45, No. 6, 926–935, June 1997.
9. Caorsi, S. and M. Pastorino, "Scattering by multilayer isorefractive elliptic cylinders," *IEEE Trans. on Antennas and Prop.,* Vol. 52 No. 1, 189–196, Jan. 2004.
10. Uslenghi, P., "Exact scattering by isorefractive bodies," *IEEE Trans. on Antennas and Prop.,* Vol. 45, No. 9, 1382–1385, Sept. 1997.
11. Jarem, J., "Rigorous coupled wave analysis of radially and azimuthally-inhomogeneous, elliptical, cylindrical systems," *Progress in Electromagnetic Research,* PIER 34, 89–115, 2001.
12. Jarem, J., "Validation and numerical convergence of the Hankel-Bessel and Mathieu rigorous coupled wave analysis algorithms for radially and azimuthally-inhomogeneous, elliptical, cylindrical systems," *Progress in Electromagnetic Research,* PIER 36, 153–177, 2002.
13. Balanis, C., *Advanced Engineering Mathematics,* John Wiley and Sons, New York, NY, 1989.
14. Harrington, R., *Field Computations by Moment Methods,* MacMillan, New York, NY, 1968.
15. Hill, C. S., "Electromagnetic excitation of dielectric concentric elliptical cylinders," Masters Thesis, Dept. of Electrical and Computer Engineering, University of Alabama in Huntsville, Dec. 17, 2004.
16. Zhang, S. and J. Jin, "FORTRAN routines for computation of special functions," Programs: MTU12, MTU0, FCOEF, CVF, CVA2 at Web Site http://irislee3.ece.uiuc.edu/-jjin/routines/routines/html, Mar. 8, 01 (Programs associated with the book Computation of Special Functions, John Wiley and Sons)
17. Jarem, J. and P. Banerjee, "Bioelectromagnetics: A rigorous coupled wave analysis of cylindrical biological tissues," *Proceedings of the International Conference on Mathematics and Engineering Techniques in Medicine and Biological Sciences,* (METMBS 00), F. Valatar (Ed.), Vol. II, 467–472, Las Vegas, Nev., June 26–29, 2000.
18. Hamid, A.-K., "Iterative solution to the TM scattering by two

infinitely long lossy dielectric elliptic cylinders," *J. of Electromagn. Waves and Appl.*, Vol. 18, No. 4, 529–546, 2004.

Susan C. Hill completed a Master of Science in Engineering from the Department of Electrical and Computer Engineering, University of Alabama in Huntsville in December 2004.

John M. Jarem received his B.S.E.E, M.S.E.E., and Ph.D. degrees from Drexel University, Philadelphia, PA, in 1971, 1972, and 1975, respectively. His research interests are in optical and microwave diffraction theory and in electromagnetics. Currently John Jarem is a professor of electrical and computer engineering at the University of Alabama in Huntsville, Huntsville AL. He is a senior member of the IEEE.